Available online at http://www.journalcra.com

International Journal of Current Research
Vol. 6, Issue, 12, pp.10413-10419, December, 2014

INTERNATIONAL JOURNAL OF CURRENT RESEARCH

ISSN: 0975-833X

REVIEW ARTICLE

EFFECT OF ANNEALING TEMPERATURE ON STRUCTURAL AND OPTICAL PROPERTIES OF ZNO NANOPARTICLES SYNTHESIZED BY SOLGEL-COMBUTION ROUTE

[1*]Bodke M. R., [2]Gaikwad H. K. and [3]Sonawane T. B.

[1]Assistant Professor Dept. of Electronic Science, Modern College of Arts, Science and Commerce Shivajinagar, Pune, Maharashtra, India
[2]Assistant Professor, Department of Chemistry, Modern College of Arts, Science and Commerce Shivajinagar, Pune, Maharashtra, India
[3]Research Scholar, Dept. of Electronics, Shivaji University, Kolhapur, Maharashtra, India

ARTICLE INFO

Article History:
Received 07th September, 2014
Received in revised form
15th October, 2014
Accepted 07th November, 2014
Published online 27th December, 2014

Key words:
Nanoparticles,
Solgel-combution,
Annealing temperature,
Hexagonal wurtzite.

ABSTRACT

ZnO nanoparticles were synthesized successfully by solgel-combution route at room temperature. X-ray diffraction (XRD) and UV-Visible spectroscopy were used to investigate the effect of annealing temperature on the structural and optical properties of ZnO nanoparticles. XRD study estimated that prepared samples had a hexagonal wurtzite structure and crystallite size 4.22 nm and 5.68 nm for ZnO nanoparticles without annealing and annealed at 600^0C temperature, formation of quantum dots observed. Optical study revealed the blue shift in energy band gap. Investigation of chemical groups and chemical bonding was completed by FTIR technique.

INTRODUCTION

Nanoparticles of the semiconductors have attracted much attention due to their novel optical, electrical and mechanical properties, which result from quantum confinement effects compared with bulk materials (Chen *et al*., 2011) ZnO is one of the promising diamagnetic semiconductor having direct band gap 3.37 eV and exciton binding energy 60 meV at room temperature. From last two decades the researchers have more attention towards ZnO nanoparticles because of its interesting properties such as photoelectric, piezoelectric and optical properties and their applications in optoelectronics (Furdyna, 1988) and (He *et al*., 2005), like Ultraviolet and blue LED's (Abiyasa *et al*., 2007), LASER diodes (Comini *et al*., 2010) (Al-Hardan *et al*., 2012) and UV sensors (Wei *et al*., 2011). Properties of ZnO are highly dependent on the preparation route used and conditions at the time of preparation too. There are various preparation routes used for the preparation of ZnO nanoparticles are described in the literature such as such as a hydrothermal method (Zhang *et al*., 2002), sol-gel (Lee *et al*., 2009).

Corresponding author: Bodke, M. R.
Assistant Professor Dept. of Electronic Science, Modern College of Arts, Science and Commerce Shivajinagar, Pune, Maharashtra, India.

Recently, ZnO nanoparticles were prepared by ultrasound (Khorsand *et al*., 2013), microwave-assisted combustion method (Kooti *et al*., 2013), two-step mechanochemical-thermal synthesis (Rajesh *et al*., 2012), anodization (Shetty *et al*., 2012), co-precipitation route (Kooti *et al*., 2013) and modified sol-gel combustion route (Zak *et al*., 2011).

In this present work ZnO nanoparticles were synthesized successfully by solgel-combusion route. We tried to study the effect of annealing temperature on the structural and optical properties of ZnO nanoparticles by using X-ray diffraction spectroscopy and UV-Visible spectroscopy techniques. Chemical species present in the sample were identified by FTIR spectroscopy.

Experimental

Chemicals used for synthesis of ZnO nanoparticles were of analytical reagents (A. R.) grade. Zinc nitrate and N-N Dimethyl formamide (N-NDMF) with their appropriate weights were added together. This mixture was stirred continuously for 2h at 70^0C temperature to get completely dissolved solution. Then the clear solution was kept on hot plate at 170^0C for 3h to form jel. Further heating of the solution combustion takes place and the ZnO nanomaterials are formed. For getting uniform crystallite size the sample was grind for 15min. The material was annealed at 600^0C.

Structural Study

The XRD pattern of ZnO nanoparticles without annealing and annealed at 600^0C are as shown in figure 1 (a) and (b). Diffraction peaks corresponds to the lattice planes for ZnO nanoparticles without annealing synthesized via solgel-combution route were (100), (002), (101), (102), (110), (103), (200), (112), (201), (004) and (202). The six peaks detected for ZnO nanoparticles annealed at 600^0C were (100), (002), (101), (102), (110), (110) and (103). XRD diffraction data compared with JCPDS card and it was well matched with JCPDS card no. (75-1526 a = 3.22 and c = 5.2), it confirms that the nanoparticles are having hexagonal (wurtzite) structure. It was reported in the literature that the diffraction peaks became sharper and the crystallite size increased with increasing annealing temperature (Yang *et al*., 2009) (Talaat *et al*., 2010) (Zak *et al*., 2011). In this study diffraction peaks estimated for the sample annealed at 600^0C were Sharper, less in numbers and shifted to the higher values of 2θ as well, indicating an enhancement of crystallinity. (2010) reported that as annealing temperature increased above 180^0C the particle morphology changed from spherical to a hexagonal shape. But in this study even though the sample was annealed at 600^0C the particle morphology remains hexagonal in shape. Lattice constants 'a', 'b' and lattice parameters crystallite size, X-ray density, volume of unit cell, APF, u-parameter and bond length were calculated from XRD data and enlisted in Table 1. The lattice constants 'a' and 'b' are closer to JCPDS card values and the blue shift is observed for ZnO nanoparticles without annealing and annealed at 600^0C. The crystallite size of ZnO nanoparticles was estimated from X-ray diffraction data using Debye-Scherrer formula (Al-Hardan *et al*., 2012),

$$D = \frac{K\lambda}{\beta \cos\theta} \quad \text{..... (1)}$$

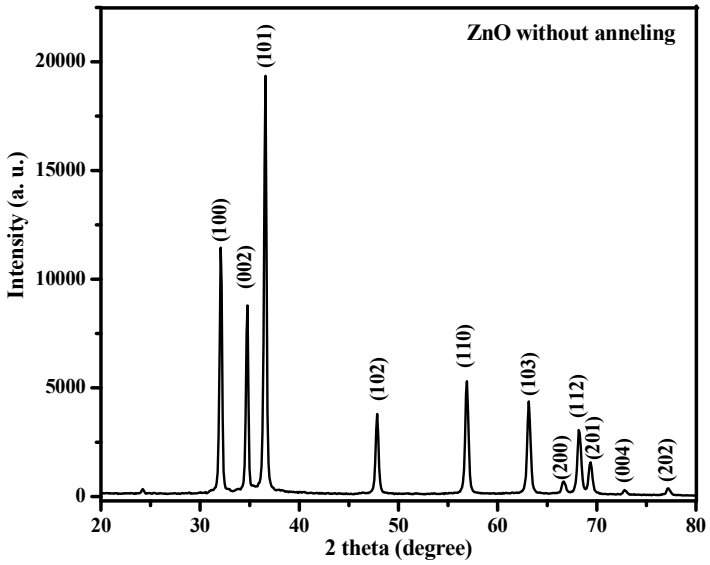

(Fig. 1) (a) XRD pattern of ZnO nanoparticles without annealing.

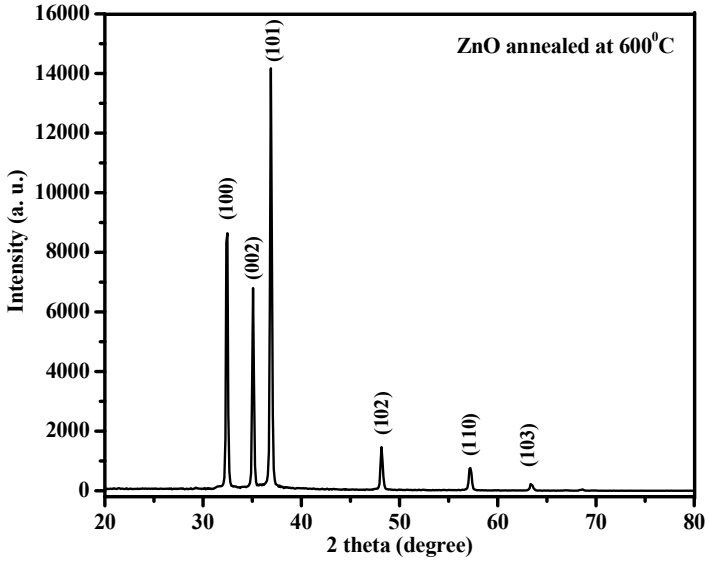

(Fig. 1) (b) XRD pattern of ZnO nanoparticles annealed at 600^0C.

Table 1. Lattice constants and lattice parameters of ZnO nanoparticles without annealing and annealed at 600^0C

Samples	Lattice constants			Lattice parameters					
	'a' (nm)	'c' (nm)	a/c ratio	Crystallite Size (nm)	X-ray density (gm/cm^3)	Volume of unit cell $(A^0)^3$	% APF	u parameter	Bond length
Nanoparticles of ZnO without annealing	3.2306	5.1809	0.6235	4.2257	5.8109	46.5266	75.36	0.3796	1.9631
Nanoparticles of ZnO annealed at 600^0C	3.1996	5.1129	0.6257	5.6807	5.9643	45.3304	75.63	0.3805	1.9135

Crystalitte sizes of ZnO nanoparticles estimated at the highest intensity peaks were 4.2257 nm and 5.6807 nm. Crystallite size of the annealed ZnO nanoparticles was greater than the ZnO nanopartices without annealing. It may be the effect of annealing temperature. X-ray density and volume of unit cell was decreased for ZnO nanoprticles from ZnO nanoparticles without annealing and the annealed nanoparticles at 600^0C. Atomic packing fraction value was slightly increased for annealed ZnO nanoparticles. Both the atomic packing fraction values are more than the reported values of bulk ZnO. The ond length 'L' of Zn-O is given by,

$$L = \sqrt{\left(\frac{a^2}{3} + \left(\frac{1}{2} - u\right)^2 c^2\right)} \quad \text{..... (2)}$$

Where 'u' is given by (in hexagonal structure) and which is related to the a/c ratio.

$$u = \frac{a^2}{3c^2} + 0.25 \quad \text{..... (3)}$$

The Zn-O bond length was decreased from 1.9631A^0 to 1.9135 A^0 for ZnO nanoparticles without annealing to the annealed ZnO nanoparticles at 600^0C temperature. It was due to decrease in the lattice constants values.

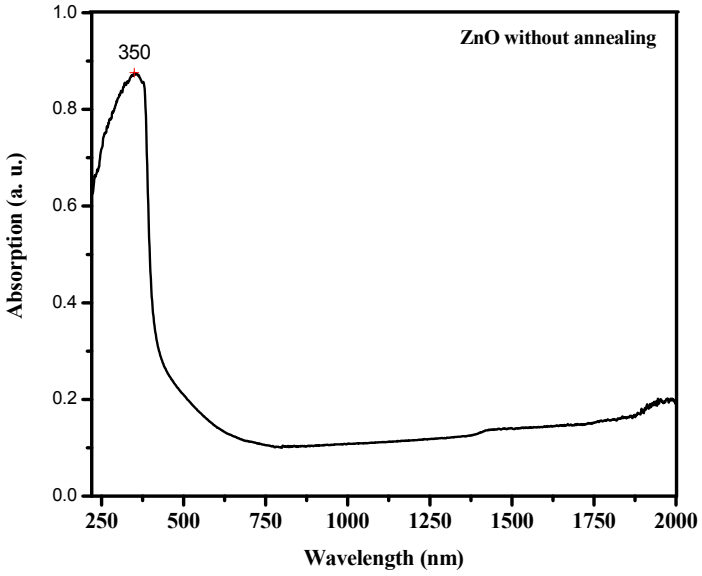

(Fig. 2) (a) Absorption spectra of ZnO nanoparticles without annealing.

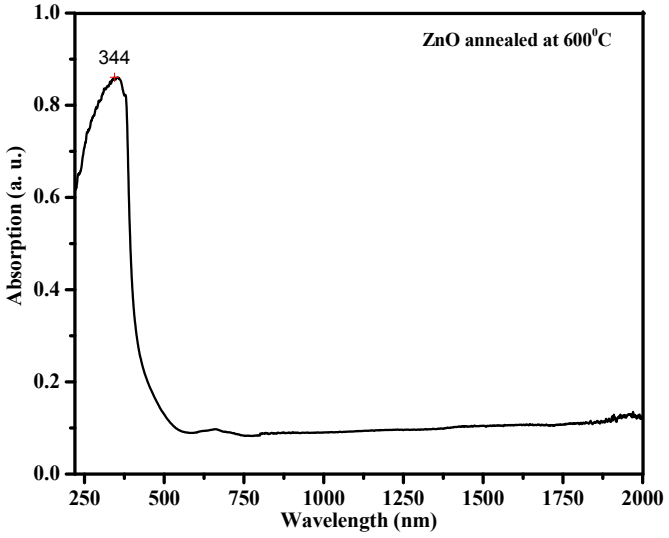

(Fig. 2) (b) Absorption spectra of ZnO anoparticles annealed at 600^0C.

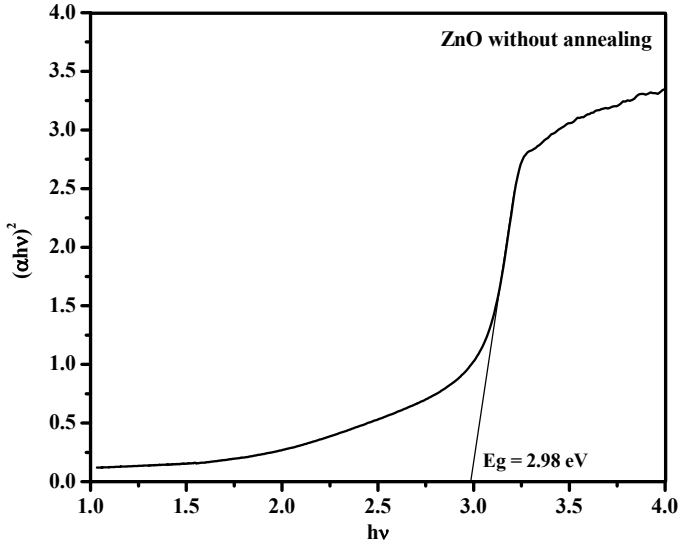

(Fig. 3) (a) Tauc's plot hν Vs $(\alpha h\nu)^2$ of ZnO nanoparticles without annealing.

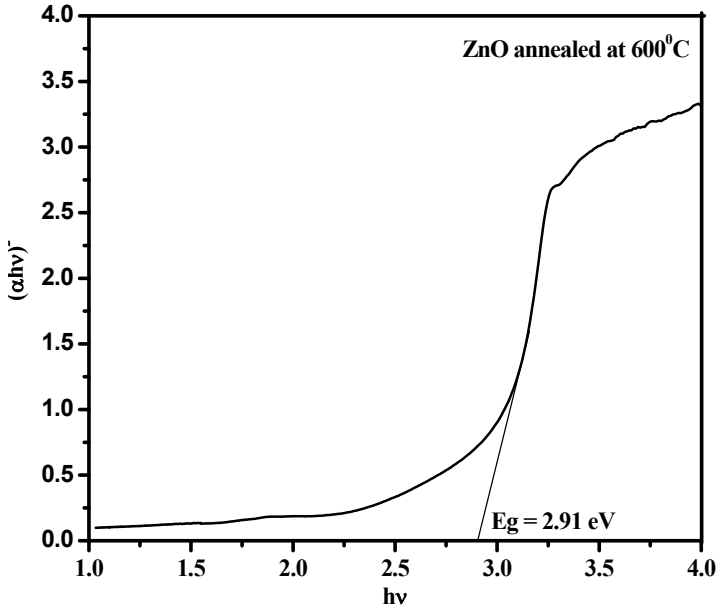

(Fig. 3) (b) Tauc's plot hν Vs (αhν)2 of ZnO nanoparticles annealed at 600^0C.

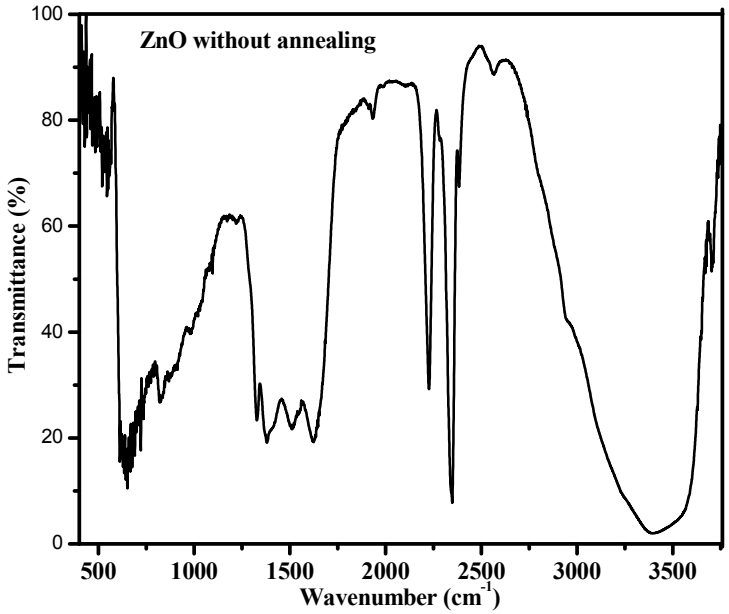

(Fig. 4) (a) FTIR spectra of ZnO nanoparticles without annealing.

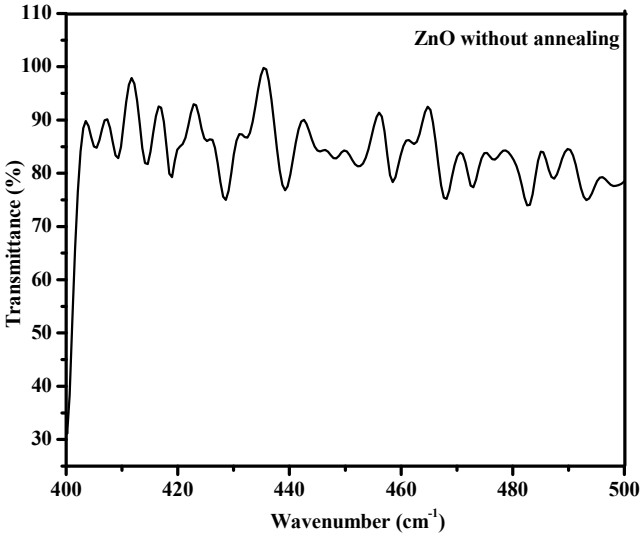

(Fig. 4) (b) FTIR spectra in between 400-500 cm^{-1} wave numbers.

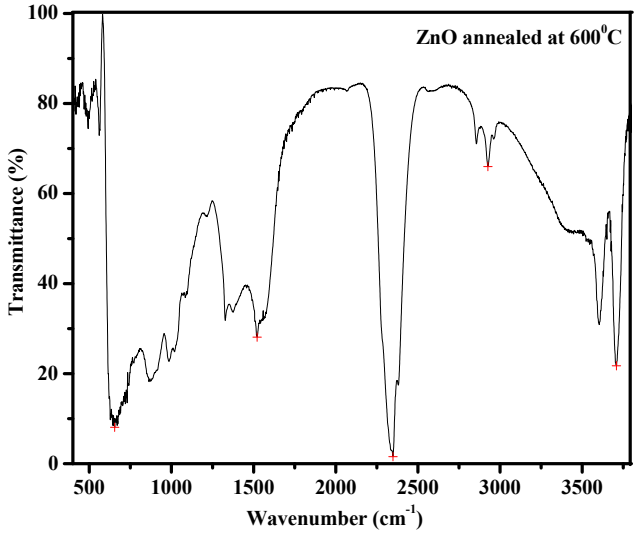

(Fig. 5) (a) FTIR spectra of ZnO nanoparticles annealed at 600^0C

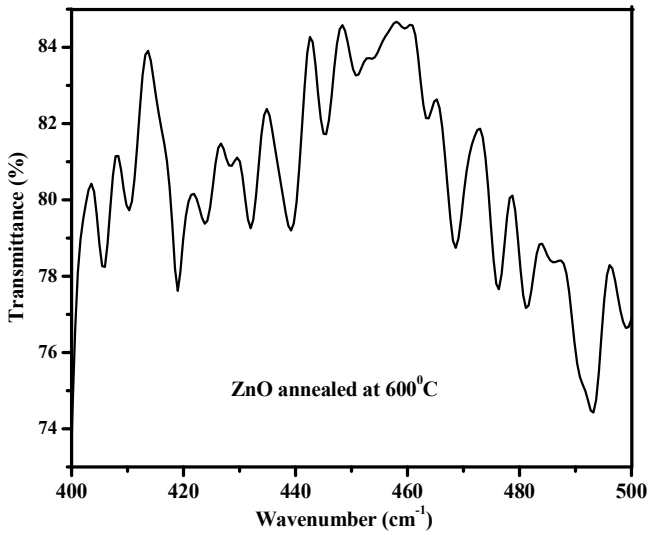

(Fig. 5) (b) FTIR spectra in the range of wave numbers 400-500 cm^{-1}.

Optical study

Optical study of Annealed ZnO nanoparticles and Zno nanoparticles without annealing has been completed using UV-Visible spectroscopy. Figure 2 (a) and (b) shows the absorption spectra for ZnO nanoparticles without annealing and the sample annealed at 600^0C. As Amor Sayari *et al.* (2013) reported that in the absorption spectra of ZnO nanoparticles a single absorption peak confirms the purity of the prepared sample. In this present work, the absorption peaks detected for ZnO nanoparticles without annealing and after annealing were at 350nm and 344nm respectively. Yu *et al*. (2006) reported that the increase in absorption less than 400 nm wavelengths can be assigned to the intrinsic band gap absorption of ZnO due to the electron transitions from the valance band to conduction band. The red shift in optical energy band gap was observed with an increase in annealing temperature (Talaat *et al*., 2010) (Zak *et al*., 2011). In this experiment, there was decrease in the value of absorption peak value from bulk ZnO to the ZnO nanoparticles sample without annealing and annealed at 600^0C. It clearly exhibits the blue shift relative to the value 375 nm of bulk ZnO (Wu *et al*., 2007). It might be quantum confinement effect and the effect of annealing temperature.

The energy band gap was determined from Tauc's plots for ZnO nanoparticles without annealing and after annealing as shown in figure 3 (a) and (b). The energy band gap intervened from hν vs $(\alpha h\nu)^2$ plots are 2.98 eV and 2.91 eV respectively. This is smaller than the energy band gap 3.37 eV of bulk ZnO and it decrease from the ZnO nanoparticle sample without annealing to the annealed ZnO nanoparticle sample. It was demonstrated that the blue shift. It may be owing to quantum confinement effect and the annealing temperature effect. The absorption peak value and the energy band gap values of ZnO nannoparticles without annealing and annealed at 600^0C temperature are smaller than the values reported in the literature.

Chemical groups and chemical bonding study

FTIR (JASCO FTIR-4100, JAPAN) spectra's were recorded at room temperature to establish the presence or absence of the various vibrational modes present in ZnO nanoparticles and to study the effect of annealing temperature on nanoparticles. Figure 4 (a) and (b) shows the FTIR spectra for ZnO nanoparticles without annealing. Figure 5 (a) and (b) shows the FTIR spectra for ZnO nanoparticles annealed at 600^0C. The broad band formed around 3400 cm^{-1} in ZnO nanoparticles without annealing was typically due to stretching and bonding modes of hydroxyl (O-H) group of H_2O(Kooti *et al*., 2013). But this broad band was shifted to the higher wave number and divided into two bands around 3597 cm^{-1} and 3708 cm^{-1}. IR absorption peaks were observed around 2219 cm^{-1}, 2348 $cm^{-1}$and 2345 cm^{-1} for ZnO nanoparticles without annealing and annealed at 600^0C temperature. The additional weak band and shoulders at 2926 cm^{-1}, 2345 cm^{-1} and 1622 cm^{-1}may be due to the quantum confinement effect. In FTIR spectra for ZnO nanoparticle without annealing, the IR peak observed around 650 cm^{-1} was due to asymmetric bending. The Five peaks were observed for ZnO nanoparticles without annealing in region 419 cm^{-1} to 482 cm^{-1} are due to Zn-O vibrational modes, where as six peaks were observed in the region around 419 cm^{-1} to 493 cm^{-1} for the ZnO nanoparticle sample annealed at 600^0C temperature. From the FTIR spectra of ZnO nanoparticle sample, it reveals that the moisture is completely removed from the sample and no effect of annealing on Zn-O vibrational mode (Nyquist, 1997) (He *et al*., 2005).

Conclusion

Nanoparticles of ZnO were synthesized by solgel-combution route. The XRD analyses clearly indicate that formation of highly pure ZnO nanoparticles. Particles morphology remains hexagonal in structure for ZnO nanoparticles without annealing and after annealing at 600^0C. The crystallite size of annealed particles increased from 4.22 nm to 5.68 nm and the absorption shifted to lower wavelengths from 350 nm to 344 nm. It exhibits the blue shift relative to the value 375 nm of bulk ZnO. The UV-visible spectra showed a blue-shift from 2.98 eV to 2.91 eV when the ZnO nanoparticles were annealed at 600^0C temperature, which were smaller than the reported values in literature. FTIR revealed the additional weak band and shoulders at 2926 cm^{-1}, 2345 cm^{-1} and 1622 cm^{-1}, it might be due to the quantum confinement effect.

REFERENCES

Abiyasa, A. P., Yu, S. F., Lau, S. P., Leong, E. S. P. and Yang, H. Y. 2007. Applied Physics Letters 90, 231106-231113.

Al-Hardan, N. H., Abdullah, M.J., Ahmed, N. M., Yam, F. K. and Aziz, A. A. 2012. Superlattice and Microstructures 51, 765-771.

Chen, C., Yu, B., Liu, P., Liu, J. F. and Wang, L., 2011. *Journal of Ceramic Processing Research*, 12, 420-425.

Comini, E. and Sberveglieri, G. 2010. Materials Today 13, 36-44.

Furdyna, J. K. 1988. *J. Appl. Phys.,* 64 R29-R64.

He,Y., Sang, W., Wang, J., Wu, R., Min, J., 2005. *J. Nanopart. Res*., 7, 307.

Khorsand, Z., Abid, A., Majid, W. H., Wang, H Z, Yousefi, R., Golsheikh, M. and Ren, Z. F., 2013. Ultrasonic Sonochemistry 20, 395–400.

Kooti, M., Nagdhi Sedish, A. 2013 *Journal of Chemistry*, doi:10.1155/2013/562028.

Lee, J., Easteal, A. J., Pal, U. and Bhattacharyya, D. 2009. *Current Applied Physics*, 9, 792-796.

Lim, J. H., Kang, C. K., Kim, K. K., Park, I. K., Hwang, D. K. and Park, S. J. 2006. *Adv. Mater*., 18, 2720-2724.

Nyquist, R. A. and Kegal, R. O. 1997, Hand book of infrared and Raman Spectra of Inorganic Compounds and Organic Salts, Academic Press, San Diego.

Rajesh, D., Vara Lakshmi, B. and Sunandana, C. S., 2012. *Physica B-Cond. Mater*., 407, 4537–4539.

Sayari, A. 2013. *KONA powder and particle Journal,* No.30, 119-124.

Shetty, A. and Nanda, K. 2012. *Appl. Phys. A.,* 109, 151–157.

Talaat, M., Hammad, J., Salem, K., Roger, G. and Harrison, 2010. Superlattices and Microstructures 47, 335-340.

Wang, L., Meng, L., Teixeira, V., Song, S., Xu, Z. and Xu, X., 2009. Thin Solid Films 517, 3721-3725.

Wei, A., Pan, L. and Huang, W. 2011. *Material Science and Engineering,* B 176, 1409-1421.

Wu, L., Wu, Y., 2007. *J. Mater. Sci*., 42, 406.

Yang, J., Liu, X., Yang, L., Wang, Y., Zhang, Y., Lang, J., Gao, M. and Feng, B. 2009. *Journal of Alloys and Compounds,* 477, 632–635.

Yu, H., Yu, J., Cheng, B., Zhou, M., J. 2006. *Solid State Chem.,* 179, 349–354.

Zak, A. K., Abrishami, M. E., Abd, W. H., Majid Yousefi, R. and Hosseini, S. M., 2011. *Ceramics International*, 37, 393–398.

Zhang, J., Sun, L. D., Yin, J., Su, H., Liao, C. S. and Yan, C. 2002. *Chem. Mater.,* 14 4172-4177.

****